Dalton Transactions

ROYAL SOCIETY OF CHEMISTRY

PAPER

View Article Online
View Journal | View Issue

Cite this: *Dalton Trans.*, 2022, **51**, 15128

A ferromagnetically coupled pseudo-calixarene [Co_{16}] wheel that self-assembles as a tubular network of capsules†

Pinelopi A. Tsami,[a] Thomais G. Tziotzi,[a] Angelos B. Canaj, [b] Mukesh K. Singh, [b] Scott J. Dalgarno, *[c] Euan K. Brechin *[b] and Constantinos J. Milios *[a]

Received 5th August 2022,
Accepted 7th September 2022

DOI: 10.1039/d2dt02554j

rsc.li/dalton

Reaction of $Co(OAc)_2{\cdot}4H_2O$ and Hsal in a basic MeCN solution affords the hexadecanuclear wheel $[Co_{16}(sal)_{16}(OAc)_{16}]{\cdot}16MeCN$ (**1**·16MeCN) that displays ferromagnetic nearest neighbour exchange and has pseudo-calixarene character. Symmetry equivalent wheels self-assemble to form remarkable tubular networks of capsules in the extended structure.

Molecular wheels attract continued attention, partly due to beautiful structural aesthetics, but also because some show fascinating and potentially useful physical properties.[1] In the field of molecular magnetism, molecular wheels of 3d transition metals came into prominence in the late 1980s and early 1990s with the publication of [Cr^{III}_8] and [Fe^{III}_{10}].[2] The former has inspired the development of a large family of homo- and heterometallic Cr wheels including the first examples of odd-numbered wheels that display topological spin frustration, with potential as quantum bits in information processing.[3] The latter, and other antiferromagnetically coupled even-membered homometallic wheels are generally characterised by a diamagnetic spin ground state and display interesting quantum phenomena and spin dynamics, including tunneling of the Néel vector,[4] spin-multiplet mixing effects[5] and magnetic level repulsions.[6] The intervening years have witnessed the publication of wheels of all the 3d metals with nuclearities up to eighty four.[7] In Co^{II} chemistry[8] early examples of wheels included a dodecanuclear cluster built with a substituted pyridone[9] and an heptanuclear Anderson wheel stabilised by tripodal alcohols[10] which both display ferromagnetic exchange interactions.

The reaction between $Co(OAc)_2{\cdot}4H_2O$ and Hsal (salicylaldehyde) in a basic MeCN solution (see ESI† for full details) leads to the formation of pink single crystals after 3 days upon diffusion of Et_2O into the mother liquor. Crystals of $[Co_{16}(sal)_{16}(OAc)_{16}]{\cdot}16MeCN$ (**1**·16MeCN) were in a tetragonal cell and structure solution was performed in the *P*4/*n* space group. The asymmetric unit (ASU) contains one quarter of the formula, and symmetry expansion affords the wheel shown in Fig. 1 (Fig. S1 and S2†).

The metallic skeleton (Fig. 2) describes a single-stranded, sinusoidal [Co^{II}_{16}] wheel of approximate diameter, Co1···Co1′ = ~14.5 Å. The 'inside' of the wheel is stabilised by sixteen μ_3-, *syn*, *syn*, *anti*-OAc ligands. Eight lie in the metal plane, with four above and four below the plane. The sixteen μ-sal ligands are arranged in a similar manner on the 'outside' of the wheel. Eight μ-sal ligands are in a belt around the periphery of the wheel, whilst four are above the plane, and four below (Fig. 1). These out of plane μ-sal ligands form an interesting arrangement that is reminiscent of calixarenes,[11] presenting a shallow hydrophobic pocket as a result. The magnetic unit between nearest neighbours contains one μ-O(alkoxide), one μ-O(carboxylate) and one *syn*, *syn*-O–C–O(carboxylate). The interaction between next nearest neighbours is mediated by the *syn*, *anti*-O–C–O(carboxylate) bridge. The Co–O–Co angles subtended by the μ-O atoms are in the range ~92.1–99.5°, with the Co^{II} ions all being in distorted octahedral {CoO_6} geometries. There are multiple close intermolecular interactions between neighbouring wheels mediated by the sal/OAc ligands with C(H)···C distances ≥3.3 Å.

A search of the Cambridge Structural Database (CSD) reveals approximately twenty [Co_{16}] structures, with more than half being squares and tetrahedra stabilised by thia- and sulfonyl-calix[4]arenes.[12] There are two other wheels, one comprising linked squares and cubes built with a bis-benzimidazolediol ligand, and one incorporating four linear {Co_4} subunits constructed with polytriazolate ligands.[13]

[a]*Department of Chemistry, The University of Crete, Voutes, 71003 Herakleion, Greece. E-mail: komil@uoc.gr*
[b]*EaStCHEM School of Chemistry, The University of Edinburgh, Edinburgh, EH9 3FJ, Scotland, UK. E-mail: ebrechin@ed.ac.uk*
[c]*Institute of Chemical Sciences, Heriot-Watt University, Riccarton, Edinburgh, EH14 4AS, UK. E-mail: S.J.Dalgarno@hw.ac.uk*

†Electronic supplementary information (ESI) available: Synthetic procedures, X-ray data and computational methodology. CCDC 2178060. For ESI and crystallographic data in CIF or other electronic format see DOI: https://doi.org/10.1039/d2dt02554j

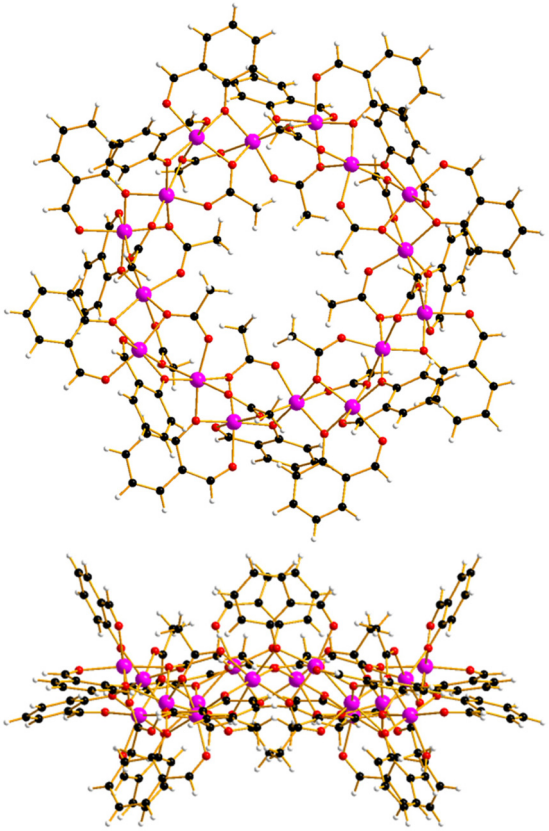

Fig. 1 Orthogonal views of the molecular structure of complex **1** viewed perpendicular (top) and parallel to the [Co_{16}] 'plane'. Colour code: Co = pink, O = red, C = black, H = white.

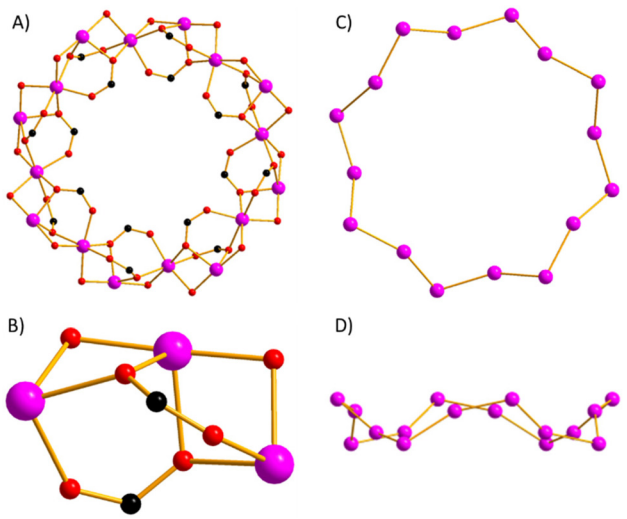

Fig. 2 (A) The magnetic core of **1**. (B) Close-up of the bridging between neighbouring Co^{II} ions. The metallic core viewed perpendicular (C) and parallel (D) to the [Co_{16}] 'plane'. Colour code: Co = pink, O = red, C = black.

Further symmetry expansion of the new pseudo-calixarene structure presented by **1** reveals a remarkable arrangement in which symmetry equivalent (s.e.) wheels pack to form tubular networks of capsules, and channels between the tubules. Inspection of the ring structure of **1** in space filling representation (Fig. 3A, in the *ab* plane) shows a very small channel through the ring as a result of the *syn*, *syn*, *anti*-OAc ligands on the inside of the molecule. Symmetry expansion along the *c* axis gives rise to a dimer with the next s.e. wheel as shown in Fig. 3B (in the *ac* plane). These pseudo-calixarene wheels lock together in the solid state through inter-digitation of the μ-sal ligands, with some OAc ligands also forming part of the space filling belt. This gives rise to an encapsulated space with a volume of ~272 $Å^3$ that is occupied by disordered solvent molecules (Fig. 3C).[14] It was not possible to resolve this disorder given the high symmetry and diffuse nature of the electron density. Inter-digitation continues along the *c* axis,

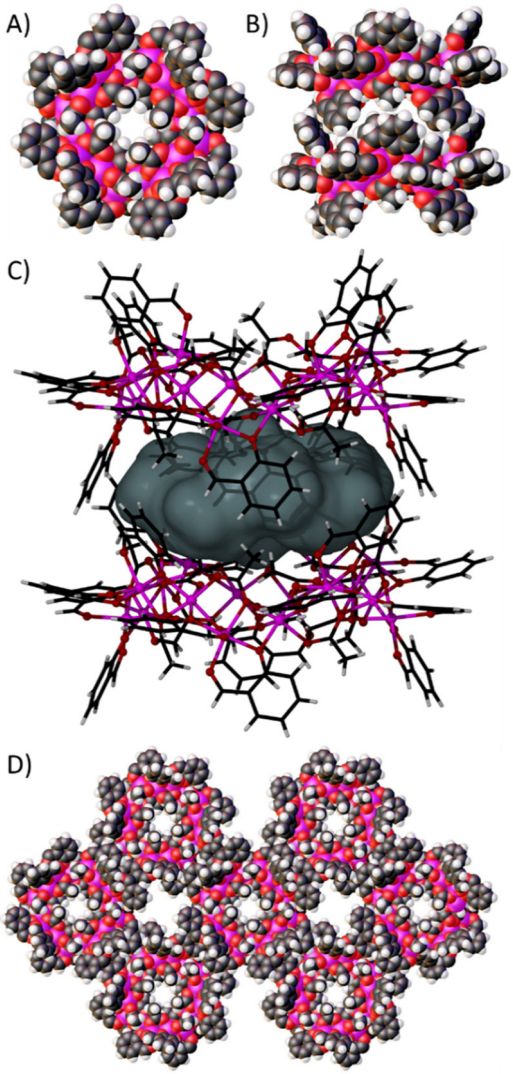

Fig. 3 Space filling representations of **1** (A, in the *ab* plane) and two symmetry equivalents interdigitating to form a cage (B, in the *ac* plane). (C) Representation of the encapsulated space between [Co_{16}] dimers with a volume of ~272 $Å^3$ occupied by disordered solvent molecules. (D) The extended structure showing the formation of channels by packing of infinite stacks of s.e. of **1** (in the *ab* plane). Colour code: Co = pink, O = red, C = black, H = white.

forming infinite tubular stacks of capsules, and these pack as shown in Fig. 3D to form solvent filled channels that run parallel through the extended structure. Single crystals of **1** are solvent dependent, but the nature of the extended structure will be studied further with a view to forming more stable analogues that can be desolvated and explored for potential guest transport to the interior of the cages.

DC magnetic susceptibility (χ) and magnetisation (M) measurements of **1** were taken in the T = 300–2.00 K, B = 0.1 T and T = 2.0–10 K and B = 0.5–9.0 T temperature and field ranges, respectively. These are plotted as the χT product *versus* T and M *versus* B in Fig. 4. The T = 300 K value of χT = 43.2 cm^3 K mol^{-1} is equal to the value expected for sixteen non-interacting S = 3/2 Co^{II} ions with g = 2.40. Upon cooling the χT value decreases slowly to ~41.7 cm^3 K mol^{-1} at 38 K before rising sharply to a maximum of ~52.8 cm^3 K mol^{-1} at T = 6 K, and then falling to ~10.9 cm^3 K mol^{-1} at T = 2 K. The initial drop in χT is due to the magnetic anisotropy of the octahedral Co^{II} ions,[15] while the increase at low temperature is due to weak ferromagnetic interactions. The drop in value between 6–2 K is most likely due to intermolecular antiferromagnetic interactions. This behaviour is similar to that observed for the pyridone-stabilised [Co$_{12}$] wheel.[9] The M *vs.* B data is in agreement with this interpretation, with the magnetisation increasing rapidly with increasing field, not saturating and reaching a value of M = 33.4 μ_B at T = 2 K and B = 9 T. There are no out-of-phase (χ'') signals in ac susceptibility measurements down to T = 2 K and frequencies up to 3000 Hz. The ferromagnetic exchange in **1** is consistent with magneto-structural correlations developed for O-bridged Co^{II} clusters where the sign and magnitude of the interaction is dictated by the Co–O–Co angle, with the exchange becoming more ferromagnetic with decreasing angle.[16] Here, the Co–O–Co angles are all ≤99.5° and are therefore expected to mediate weak ferromagnetic exchange.

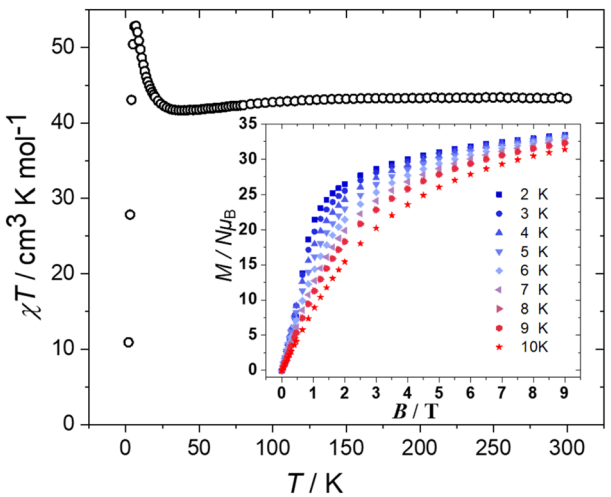

Fig. 4 Plot of the χT product *versus* T in the range T = 300–2 K in an applied field, B = 0.1 T. Inset: plot of the M *versus* B data in the T = 2.0–10 K and B = 0.5–9.0 T temperature and field ranges, respectively.

In order to probe the nature and magnitude of the magnetic exchange and anisotropy of the Co^{II} ions further, we now turn to theory (see the computational details in the ESI† for full details).[17] We have performed DFT calculations on a model of complex **1** (**Model 1**) based on its ASU, *i.e.* one [Co$^{II}_4$] moiety plus one linking Co^{II} ion (Fig. S4†). Based on symmetry and structure there are four unique nearest neighbour magnetic exchange interactions with J values ranging between +1.7 cm^{-1} ≤ J ≤ +3.8 cm^{-1} (Table S2†). The narrow range of ferromagnetic exchange interactions found can be attributed to the similarity of the structural parameters present, including the average Co–μO–Co angles.[16] We have also performed overlap integral calculations[17] using the singly occupied molecular orbitals (SOMOs) of the Co^{II} ions (Fig. S5†). These help to elucidate the magnitude and sign of magnetic interactions since their magnitude is directly proportional to the magnitude of the antiferromagnetic interaction, *i.e.* the larger the overlap the larger the antiferromagnetic interaction and *vice versa*. For **1**, there are three intermediate and six small overlap interactions, resulting in a small ferromagnetic interaction overall. Interestingly, replacement of the phenoxide group in **Model 1** with a point charge changes the sign of the magnetic interaction from ferromagnetic to antiferromagnetic (+4.2 cm^{-1} to −3.4 cm^{-1}), highlighting the importance of this moiety for obtaining ferromagnetic exchange. We have also calculated the next-nearest neighbour exchange mediated *via* the *syn*, *anti*-O–C–O(carboxylate). These are weak and antiferromagnetic, with J < −0.2 cm^{-1} (Fig. S6†).

All the Co^{II} ions in **1** are in distorted octahedral geometries (Table S3†), with previous magneto-structural studies suggesting such ions would possess large easy-plane anisotropy.[18] *Ab initio* NEVPT2 calculations on each Co^{II} ion in **1** confirms this, with values in the range +41.2 ≤ D ≤ +87.1 cm^{-1}. The dominant contribution to D arises from the $d_{xz/yz} \rightarrow d_{xy}$ electronic transition (Table S4, Fig. S7†). Positive axial zero-field splitting can be attributed to electronic transitions between orbitals with different m_L values and the magnitude correlated to the energy separation between the orbitals involved in the electronic transition.[19] The computed D_{zz} axes for Co1–Co4 are shown in Fig. S8† and are non-collinear, primarily due to the sinusoidal arrangement of metal centres. This is likely also the reason **1** is not an SMM. We also note that $|D| \gg |J|$ and in such scenarios an isotropic description of the exchange should be regarded with some caution.[20]

In summary, the reaction of Co(OAc)$_2$·4H$_2$O and Hsal affords the aesthetically pleasing [Co$_{16}$(μ-sal)$_{16}$(μ$_3$-OAc)$_{16}$] (**1**) wheel, which displays weak ferromagnetic nearest neighbour exchange interactions, in agreement with DFT calculations. *Ab initio* NEVPT2 studies suggest the presence of large single ion easy-plane anisotropy. In the extended structure the wheels form dimeric capsules *via* inter-digitation of the sal/acetate ions and this extends to form infinite tubular stacks of capsules upon symmetry expansion. Attempts to make analogues of **1** with different M^{II} ions, different carboxylates and derivatised salicylaldehyde ligands are in progress, with a view to also examining guest transport to the interior of the cages.

Conflicts of interest

There are no conflicts to declare.

Acknowledgements

This work was supported by the Hellenic Foundation for Research and Innovation (H.F.R.I.) under the "First Call for H. F.R.I. Research Projects to support Faculty members and Researchers and the procurement of high-cost research equipment grant" (Project Number: 400). We thank the Leverhulme Trust (RPG-2021-176) and the European Union Horizon 2020 research and innovation programme under the Marie Skłodowska-Curie grant agreement no. 832488. For the purpose of open access, the author has applied a Creative Commons Attribution (CC BY) license to any Author Accepted Manuscript version arising from this submission.

References

1 See for example: (*a*) O. Poncelet, L. G. Hubert-Pfalzgraf, J.-C. Daran and R. Astier, *J. Chem. Soc., Chem. Commun.*, 1989, 1846–1848; (*b*) H. Barrow, D. A. Brown, N. W. Alcock, H. J. Clase and M. G. H. Wallbridge, *J. Chem. Soc., Chem. Commun.*, 1995, 1231–1232; (*c*) J. S. Anderson, *Nature*, 1937, **140**, 850; (*d*) A. Müller, M. Koop, H. Bögge, M. Schmidtmann and C. Beugholt, *J. Chem. Soc., Chem. Commun.*, 1998, 1501–1502.

2 (*a*) N. V. Gerbeleu, A. S. Batsanov, G. A. Timko, Yu. T. Struchkov, K. M. Indrichan and G. A. Popovich, *Patent SU* 1299116(A1), 1989-12-15. Bull. 1989, 46. Priority numbers: SU19853940102 date 1985-08-07; (*b*) N. V. Gerbeleu, Y. T. Struchkov, G. A. Timko, A. S. Batsanov, K. M. Indrichan and G. A. Popovich, *Dokl. Akad. Nauk SSSR*, 1990, **313**, 1459–1462; (*c*) K. L. Taft and S. J. Lippard, *J. Am. Chem. Soc.*, 1990, **112**, 9629–9630; (*d*) K. L. Taft, C. D. Delfs, G. C. Papaefthymiou, S. Foner, D. Gatteschi and S. J. Lippard, *J. Am. Chem. Soc.*, 1994, **116**, 823–832.

3 See for example: (*a*) R. J. Woolfson, G. A. Timco, A. Chiesa, I. J. Vitorica-Yrezabal, F. Tuna, T. Guidi, E. Pavarini, P. Santini, S. Carretta and R. E. P. Winpenny, *Angew. Chem.*, 2016, **128**, 9002–9005; (*b*) M. Baker, T. Lancaster, A. Chiesa, G. Amoretti, P. J. Baker, C. Barker, S. J. Blundell, S. Carretta, D. Collison, H. U. Güdel, T. Guidi, E. J. L. Mcinnes, J. S. Moeller, J. H. Mutka, J. Ollivier, F. L. Pratt, P. Santini, F. Tuna, O. L. Tregenna-Piggott, I. Vitorica-Yrezabal, G. A. Timco and R. E. P. Winpenny, *Chem. – Eur. J.*, 2016, **22**, 1779–1788.

4 F. Meier and D. Loss, *Phys. Rev. Lett.*, 2001, **86**, 5373–5376.

5 S. Carretta, J. van Slageren, T. Guidi, E. Liviotti, C. Mondelli, D. Rovai, A. Cornia, A. L. Dearden, F. Carsughi, M. Affronte, C. D. Frost, R. E. P. Winpenny, D. Gatteschi, G. Amoretti and R. Caciuffo, *Phys. Rev. B: Condens. Matter Mater. Phys.*, 2003, **67**, 094405.

6 M. Affronte, A. Cornia, A. Lascialfari, F. Borsa, D. Gatteschi, J. Hinderer, M. Horvatić, A. G. M. Jansen and M.-H. Julien, *Phys. Rev. Lett.*, 2002, **88**, 167201.

7 A. J. Tasiopoulos, A. Vinslava, W. Wernsdorfer, K. A. Abboud and G. Christou, *Angew. Chem., Int. Ed.*, 2004, **43**, 2117–2121.

8 M. Murrie, *Coord. Chem. Rev.*, 2010, **39**, 1986–1995.

9 E. K. Brechin, O. Cador, A. Caneschi, C. Cadiou, S. G. Harris, S. Parsons, M. Vonci and R. E. P. Winpenny, *Chem. Commun.*, 2002, 1860–1861.

10 M. Moragues-Canovás, C. E. Talbot-Eeckelaers, L. Catala, F. Lloret, W. Wernsdorfer, E. K. Brechin and T. Mallah, *Inorg. Chem.*, 2006, **45**, 7038–7040.

11 (*a*) C. D. Gutsche, in *Calixarenes: An Introduction*, The Royal Society of Chemistry, Cambridge, 2nd edn, 2008, ch. 2, pp. 27–160; (*b*) S. T. Meally, C. McDonald, G. Karotsis, G. S. Papaefstathiou, E. K. Brechin, P. W. Dunne, P. McArdle, N. P. Power and L. F. Jones, *Dalton Trans.*, 2010, **39**, 4809–4816.

12 See for example: (*a*) M. Liu and W. Liao, *CrystEngComm*, 2012, **14**, 5727–5729; (*b*) X. Hang, S. Wang, X. Zhu, H. Han and W. Liao, *CrystEngComm*, 2016, **18**, 4938–4943.

13 (*a*) W.-Q. Lin, J.-D. Leng and M.-L. Tong, *Chem. Commun.*, 2012, **48**, 4477–4470; (*b*) Y.-Q. Hu, M.-H. Zeng, K. Zhang, S. Hu, F.-F. Zhou and M. Kurmoo, *J. Am. Chem. Soc.*, 2013, **135**, 7901–7908.

14 L. J. Barbour, *J. Appl. Crystallogr.*, 2020, **53**, 1141–1146.

15 A. Abragam and B. Bleaney, *Electron Paramagnetic Resonance of Transition Ions*, Dover Publications, New York, 1970.

16 X.-J. Song and X.-M. Xue, *ACS Omega*, 2020, **5**, 8347–8354.

17 (*a*) M. K. Singh, A. Etcheverry-Berríos, J. Vallejo, S. Sanz, J. Martínez-Lillo, G. S. Nichol, P. J. Lusby and E. K. Brechin, *Dalton Trans.*, 2022, **51**, 8377–8381; (*b*) D. J. Cutler, M. Coletta, M. K. Singh, A. B. Canaj, L. J. McCormick, S. J. Coles, J. Schnack and E. K. Brechin, *Dalton Trans.*, 2022, **51**, 8945–8948; (*c*) M. Coletta, T. G. Tziotzi, M. Gray, G. S. Nichol, M. K. Singh, C. J. Milios and E. K. Brechin, *Chem. Commun.*, 2021, **57**, 4122–4125; (*d*) D. J. Cutler, M. K. Singh, G. S. Nichol, M. Evangelisti, J. Schnack, L. Cronin and E. K. Brechin, *Chem. Commun.*, 2021, **57**, 8925–8928; (*e*) M. K. Singh and G. Rajaraman, *Inorg. Chem.*, 2019, **58**, 3175–3188; (*f*) C. McDonald, S. Sanz, E. K. Brechin, M. K. Singh, G. Rajaraman, D. Gaynor and L. F. Jones, *RSC Adv.*, 2014, **4**, 38182; (*g*) S. Hazra, S. Bhattacharya, M. K. Singh, L. Carrella, E. Rentschler, T. Weyhermueller, G. Rajaraman and S. Mohanta, *Inorg. Chem.*, 2013, **52**, 12881–12892.

18 S. Gómez-Coca, D. Aravena, R. Morales and E. Ruiz, *Coord. Chem. Rev.*, 2015, **289–290**, 379.

19 (*a*) M. K. Singh, P. Shukla, M. Khatua and G. Rajaraman, *Chem. – Eur. J.*, 2020, **26**, 464–477; (*b*) Y.-F. Deng, M. K. Singh, D. Gan, T. Xiao, Y. Wang, S. Liu, Z. Wang, Z. Ouyang, Y.-Z. Zhang and K. R. Dunbar, *Inorg. Chem.*, 2020, **59**, 7622–7630.

20 (*a*) L. F. Chibotaru, L. Ungur, C. Aronica, H. Elmoll, G. Pilet and D. Luneau, *J. Am. Chem. Soc.*, 2008, **130**, 12445; (*b*) O. Waldmann, M. Ruben, U. Ziener, P. Müller and J. M. Lehn, *Inorg. Chem.*, 2006, **45**, 6535–6540.